PS Fluvial Architecture of the Burro Canyon Formation Using UAV-Based Photogrammetry: Implications for Reservoir Performance, Rattlesnake Canyon, Southwest Piceance Basin, Colorado*

Kelsey Lewis[1], Matthew Pranter[1], Zulfiquar Reza[1], and Rex Cole[2]

Search and Discovery Article #51553 (2019)**
Posted February 25, 2019

*Adapted from poster presentation given at AAPG 2018 Annual Convention & Exhibition, Salt Lake City, Utah, United States, May 20-23, 2018
 DOI:10.1306/51553Lewis2019

[1]University of Oklahoma, Norman, OK, United States (kelsey.lewis@bpx.com)
[2]Colorado Mesa University, Grand Junction, CO, United States

Abstract

The stratigraphic variability of fluvial architectural elements and their internal lithological and petrophysical heterogeneity influence static connectivity and fluid flow. To explore the impact of fluvial architecture and facies heterogeneity on reservoir performance, we evaluated well-exposed outcrops of the Burro Canyon Formation in Rattlesnake Canyon, Colorado. Analysis of sedimentology and channel-stacking geometries of the Burro Canyon Formation provides insight into the low net-to-gross ratio braided fluvial style during the Early Cretaceous.

We used stratigraphic measured sections, thin-section petrography, outcrop gamma-ray measurements, and UAV- (Unmanned Aerial Vehicle-) based photogrammetry to constrain three-dimensional (3-D) geologic reservoir models of the fluvial deposits. Measured sections and thin- section analysis capture the sedimentology and stratigraphic variability of the fluvial sandstone bodies. We used UAV-based photogrammetry and outcrop gamma-ray measurements to classify stacking and geometry of the channel-complex systems. We used outcrop data to condition three-dimensional (3-D) geologic (static) and dynamic reservoir models using multiple scales of heterogeneity. Large-scale heterogeneity is associated with architectural elements and their geometries. Small-scale heterogeneity is related to sedimentary structures and internal fluvial sandstone variability.

With multi-scale heterogeneity captured in petrophysical property models, subsurface fluid flow is simulated under various conditions. Using a 5-spot pattern, a single injector surrounded by four producing wells, both the large- and small-scale geologic models are simulated over 30 years for both black oil and condensate gas production. Comparison of the impacts of large- and small-scale heterogeneities on reservoir fluid flow, storage capacity, and recovery provides insight into the impacts of fluvial heterogeneity on reservoir performance.

Abstract

The stratigraphic variability of fluvial architetural elements and their internal lithological and petrophysical heterogeneity influenc static connectivity and fluid flow. To explore the impact of fluvial architecure and facies heterogeneity on reservoir performance, well-exposed outcrops of the Cretaceous Burro Canyon Formation in Rattlesnake Canyon, Colorado, are evaluated. Analysis of the sedimentology and channel architecture of the Burro Canyon Formation provides insights into the low net-to-gross ratio, sandy, braided-fluvial style. The Burro Canyon Formation represents a South saskatchewan type, perennial, braided fluvial system. A single depositional sequence is present in Rattlesnake Canyon contianing a series of stacked amalgamated and semi-amalgamated channel complexes, composed of four architectural elements: amalgamated channel complexes, amalgamated fluvial-bar deposits, isolated fluvial-bar depsoits, and floodplain fines.

Stratigraphic measured sections, outcrop gamma-ray measurements, and UAV-based (Unmanned Aerial Vehicle-based) photogrammetry are used to constrain two-dimensional (2-D) and three-dimensional (3-D) static reservoir models of the fluvial deposits. Resulting breathrough times (BTT) and sweep efficiency suggest subsurface performance is most effective perpendicular to paleoflow direction in amalgamated channel sequences. Perpendicular to paleoflow, BTT occurs 9% faster than parallel to paleoflow and sweep efficiency is, on average, 16% greater. Sweep efficiency and BTT are greater perpendicular to paleoflow due to greater sandstone connectivity in this orientation, variability of preserved channels and lateral pinchouts results in lower recovery efficiency. Reservoir heterogeneity can account for 50% variation in BTT and lower recovery efficiency by 5% through low petrophysical zones that trap fluids. Cemented conglomeratic facies decrease recovery efficiency by 15%, but increase sweep efficiency and BTT by 28% and 32%, respectively, creating fluid-flow barriers as conglomeratic facies fill basal scours in the Burro Canyon Formation.

Study Area

A)

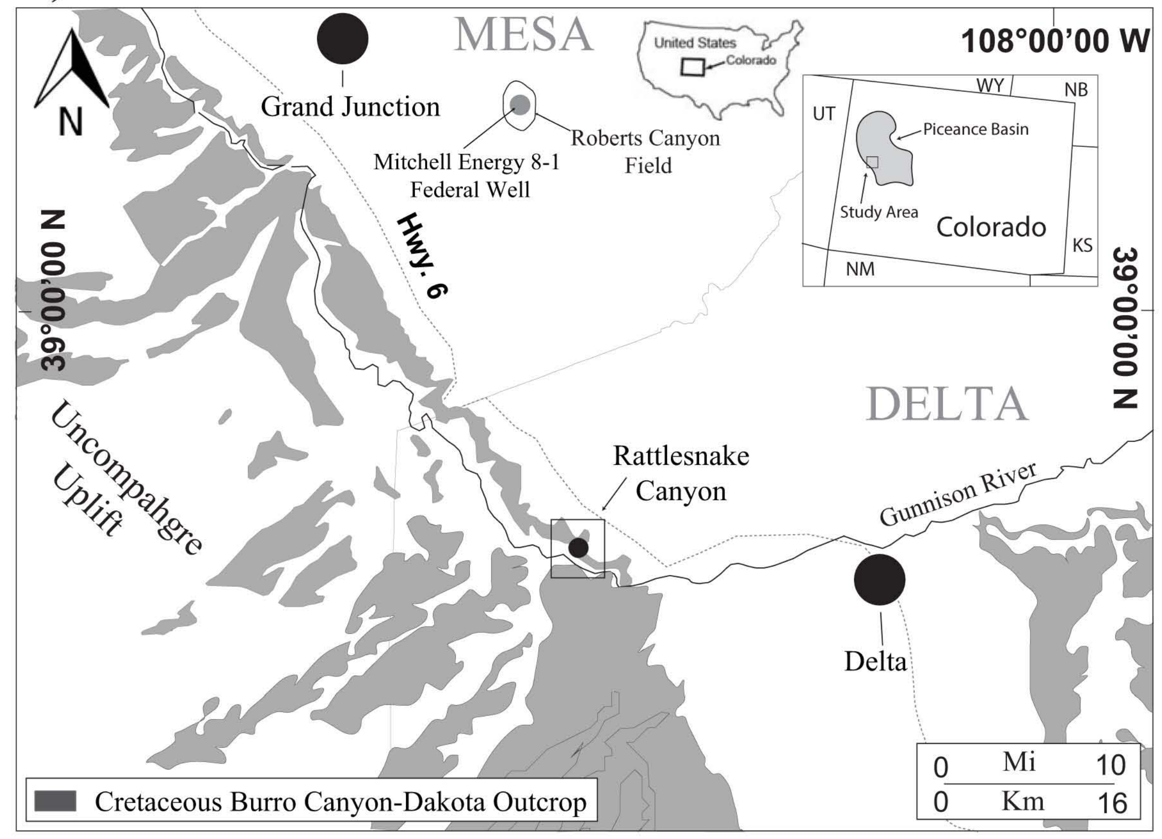

A) Study area located in the southwestern portion of the Piceance Basin, to the south of Grand Junction and west of Delta, Colorado. Dark shaded features indicate exposed outcrops of the Burro Canyon Formation.

B) Rattlesnake Canyon study area contains three exposed walls of Burro Canyon Formation. Locations of measured sections 1-3 are shown. Green shaded area indicates canyon walls imaged with a DJI Phantom 3 Drone.

C) Early Cretaceous paleomap showing location of the western interior seaway in proximity to the Piceance Basin. At this time, sediment influxes from the Sevier orogeny deposit the Burro Canyon to the northwest.

B)

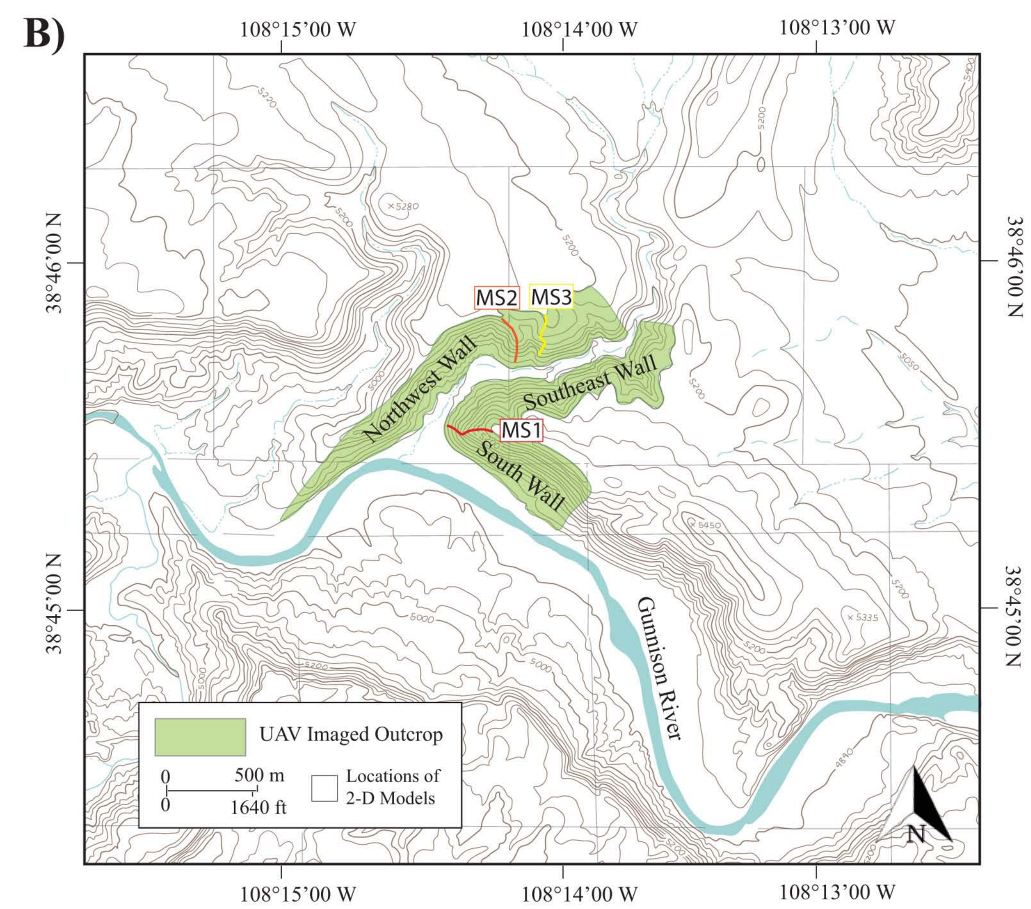

C)

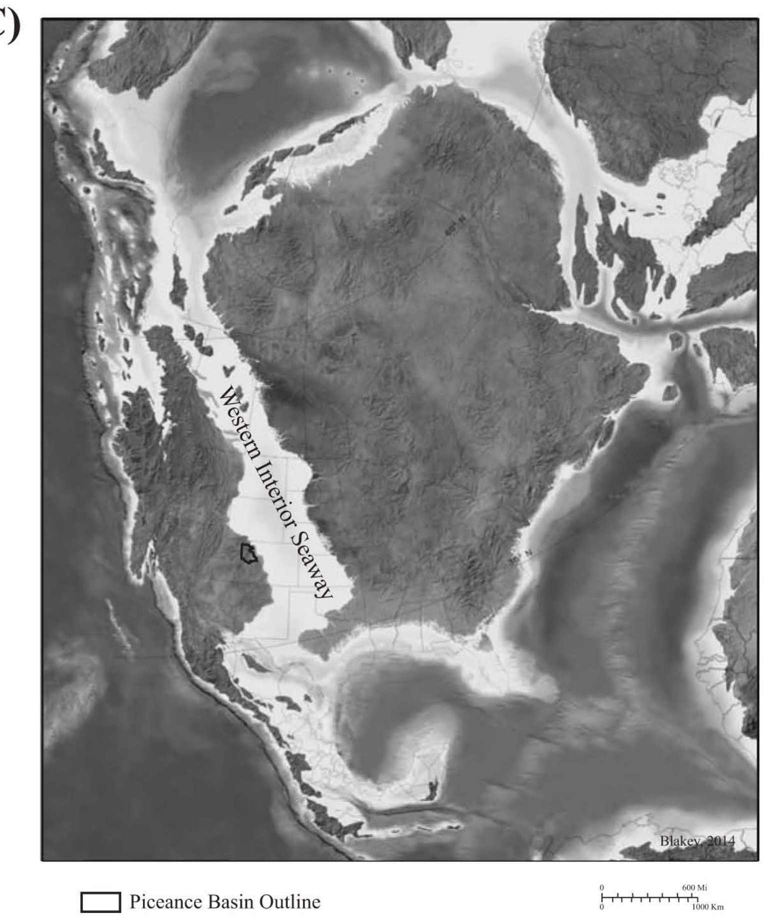

Research Questions

1. What is the sedimentology and stratigraphic hierarchy of the Burro Canyon Fromation?

2. What is the depositional envrionment for the Burro Canyon Formation?

3. What are the types and geometries of architectural elements present?

4. What is the impact of different scales of depositional heterogeneity on reservoir performance?

Workflow

Outcrop Analysis

Measured sections, outcrop samples and paleocurrent measurements obtained

UAV-Based Photogrammetry

Systematic images taken along exposed outcrop faces, capturing outcrop heterogeneity

Pix4D Outcrop Model

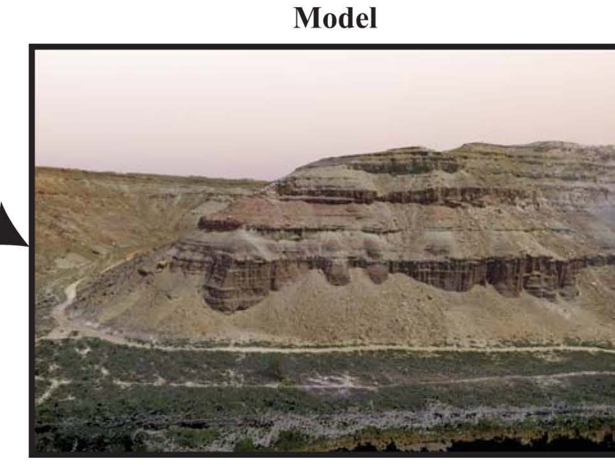

Pix4D point cloud imported into petrel. Pseudo wells created and constrained to outcrop facies along canyon walls

Petrel Outcrop Model

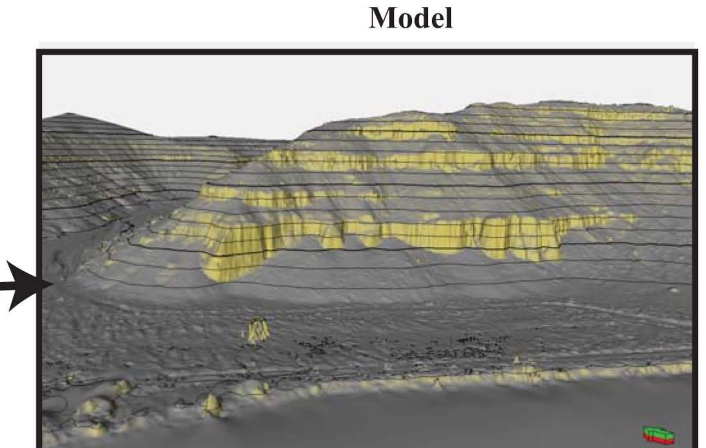

Photogrammetry data imported to create dense pointcloud and 3-D surface model of Rattlesnake Canyon. Channel geometries mapped and evaluated

Outcrop Constrained Geologic Model

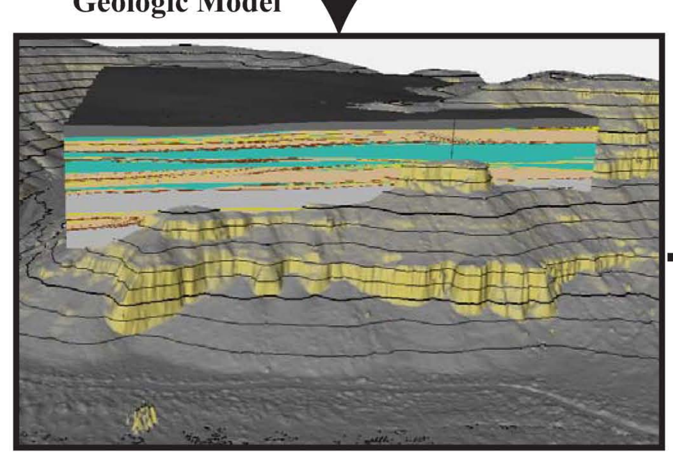

Geolgoic (static) 2-D and 3-D models are created from canyon pseudo wells and constrained to variogram data from canyon geometries

Petrophysical Model Constraints

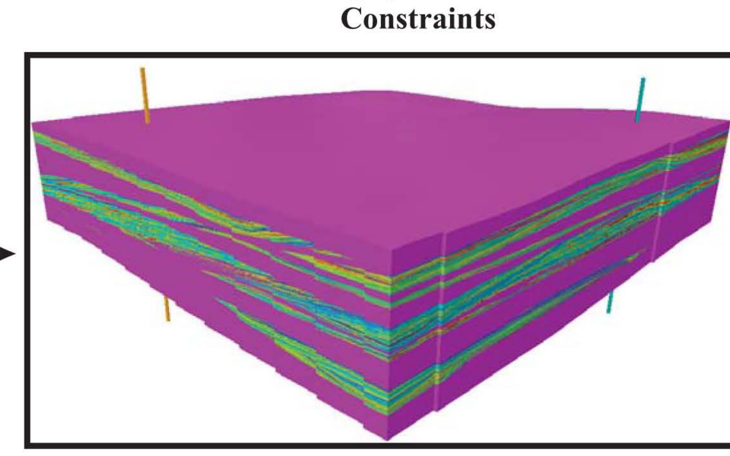

Geologic reservoir model populated with porosity and permeability values determined from core data

Simulated Reservoir Model

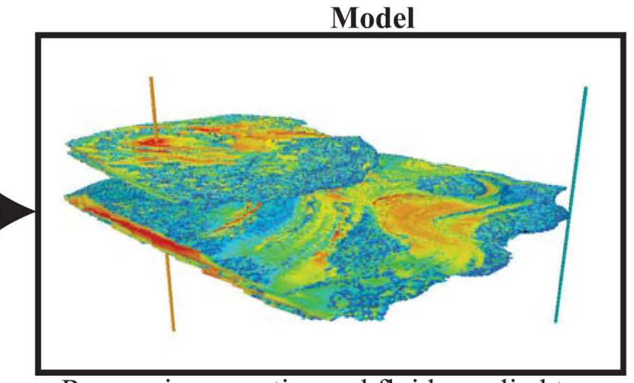

Reservoir properties and fluids applied to create dynamic reservoir models to be simulated through breakthrough time

Fluvial Architecture of the Burro Canyon Formation using UAV-Based Photogrammetry: Implications for Reservoir Performance, Rattlesnake Canyon, Southwest Piceance Basin, Colorado

The UNIVERSITY of OKLAHOMA
Mewbourne College of Earth and Energy
ConocoPhillips School of Geology and Geophysics
ConocoPhillips

Kelsey D. Lewis[1], Matthew J. Pranter[1], Zulfiquar A. Reza[2] and Rex D. Cole[3]

[1]ConocoPhillips School of Geology and Geophysics, University of Oklahoma, Norman, Oklahoma
[2]Mewbourne School of Petroleum and Geological Engineering, University of Oklahoma, Norman, Oklahoma
[3]Department of Physical and Environmental Sciences, Colorado Mesa University, Grand Junction, Colorado

RCML
Reservoir Characterization and Modeling Laboratory
The University of Oklahoma

Sedimentology

Composite measured section of the Burro Canyon Formation in Rattlesnake Canyon shown in comparison with the gamma ray log from the Mitchell Energy Federal 8-1 well. Composite measured section goes from the upper most Morrison Formation to the base of the Dakota Formation encompassing the entire Burro Canyon Formation present in Rattlesnake Canyon. Paleocurrent measurements taken throughout the Canyon give a vector mean of 58º.

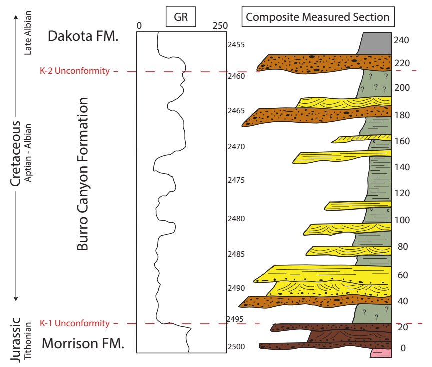

A)

Outcrop Lithofacies

Facies Code	Facies Name	Grain Size	Sorting	Stratification	Color	Cement Type	Clast Type	Thickness	Depositional Environments
A	Conglomeratic Granule-Pebble Sandstone	Granule-Pebble	Poor-Moderate	——	Dark Brown/ Tan	Calcite	Quartzite, Chert, Lithics	1-3 ft	Channel Floor Lag
B	Trough Cross-Bedded Sandstone	Fine- to Medium-Grained	Moderate - High	Trough-Cross Stratification	Light Brown/ Tan	Calcite / Silica	Quartz, Chert	1-15 ft	Cross Channel Bars and Compound Bars
C	Chert-Rich Sandstone	——	High	2-6 in laminations	Light Gray	——	Chert	2 ft	Diagenetic
D	Planar Laminated Sandstone	Very Fine- to Fine-Grained	Moderate - High	Planar Laminated	Light Brown/ Tan	Calcite	Quartz, Calcite	1-5 ft	Compound Bars
E	Structureless Sandstone	Fine- to Medium-Grained	Moderate - High	——	Light Brown/ Tan	Calcite / Silica	Quartz, Chert	1-15 ft	Cross Channel Bars and Compund Bars
F	Low-Angle Planar Laminated Sandstone	Very Fine- to Fine-Grained	Moderate - High	Low-Angle Laminated	Rust Brown	Calcite	Quartz, Calcite	1-5 ft	Compound Bars
G	Fissile Mudstone	Clay-Sized	High	Thinly Laminated	Gray-Black	Calcite	Mudstone	5-30 ft	Floodplain
H	Gray-Green Mudstone	Clay-Sized	High	Thinly Laminated	Gray-Green	Calcite	Mudstone	5-30 ft	Floodplain/ Lacustrine

Eight individual lithofacies have been identified in the Burro Canyon Formation of Rattlesnake Canyon. A) Images of eight identified lithofacies present in the Burro Canyon Formation. B) Descriptions of eight outcrop lithfacies found in Rattlesnake Canyon, depicting identifying factors such as grain size, sorting and depositional environment.

B)

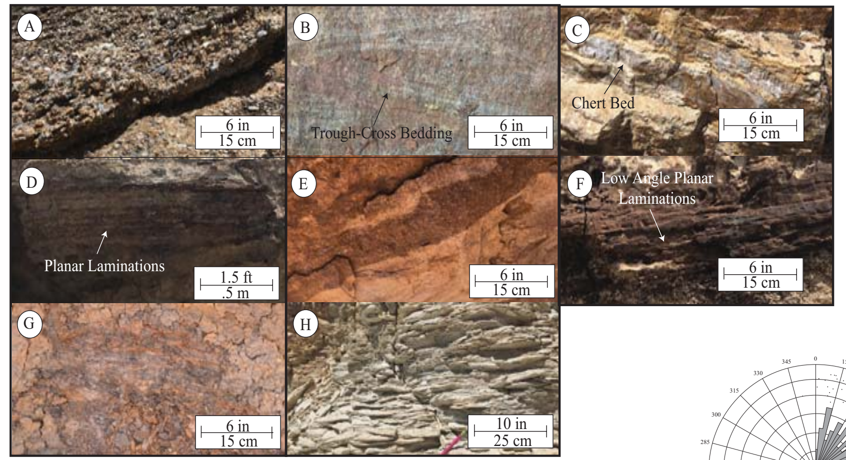

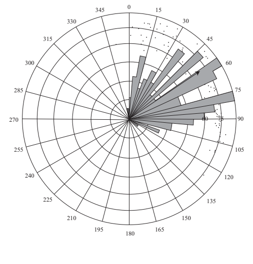

N = 124
VM = 58º

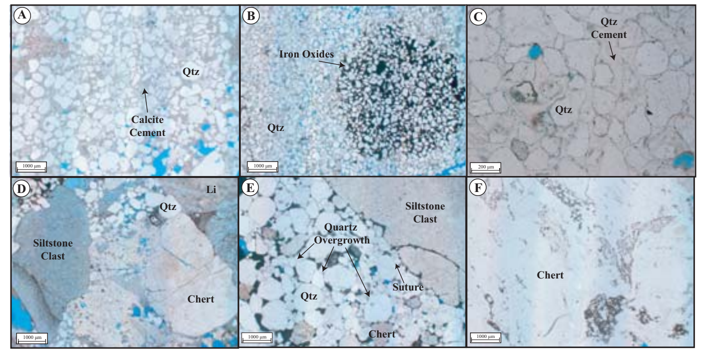

Thin section images representing lithofoacies and grains present in the Burro Canyon Formation within Rattlesnake Canyon. Framework grains largely composed of quartz, chert and calcite with conglomerates containing siltstone, chert and lithics. Cement is composed of calcite and occasionally silica. Quartz overgrowths are present trhoughout trough cross-bedded sandstone. Iron oxides are present throughout reservoir facies intervals.

Drone Modeling

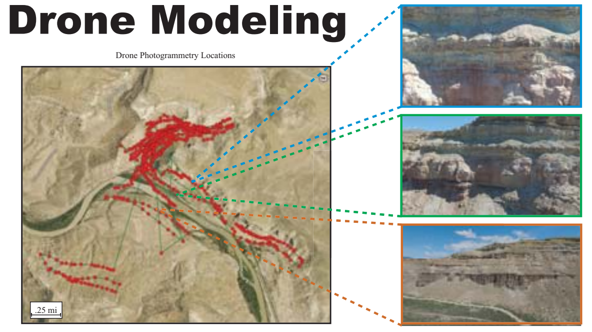

Systematic imaging of Rattlesnake Canyon was performed to ensure full 3-D coverage of the Burro Canyon Formation present. Images were taken at three distances from the outcrop to show not only geometries present but also sedimentary structures. Red dots indicate location of drone during imaging of the canyon.

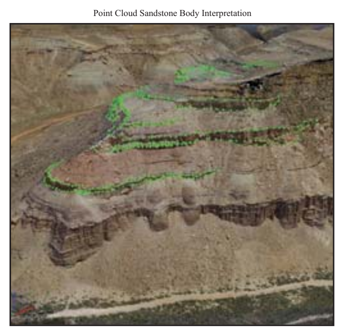

Drone images were imported into Pix4D program in order to map channels present for width, thickness and spatial relationships.

Architectural Elements

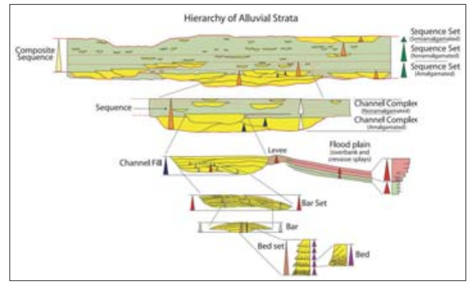

Architectural elements are defined based off of the classification scheme defined by Patterson et al. 2010, and Sprague et al, 2002.

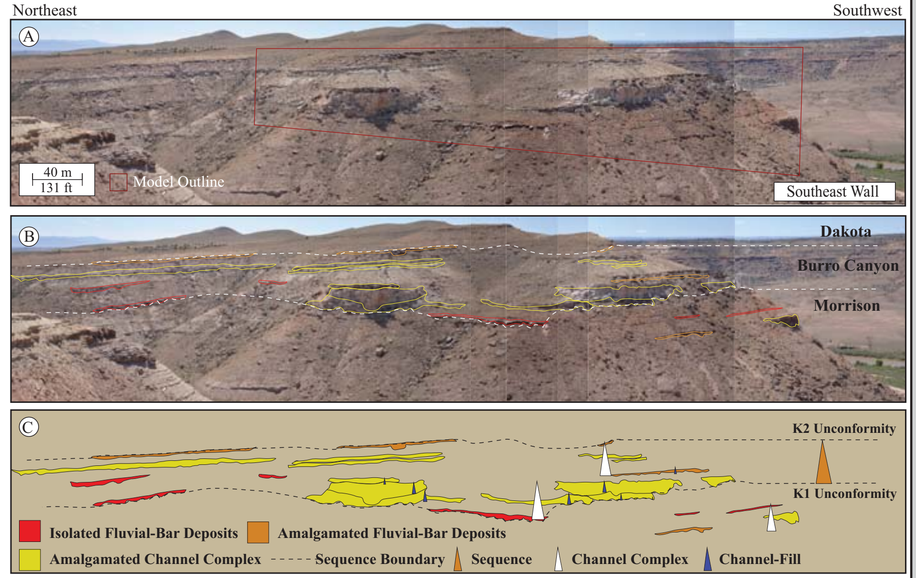

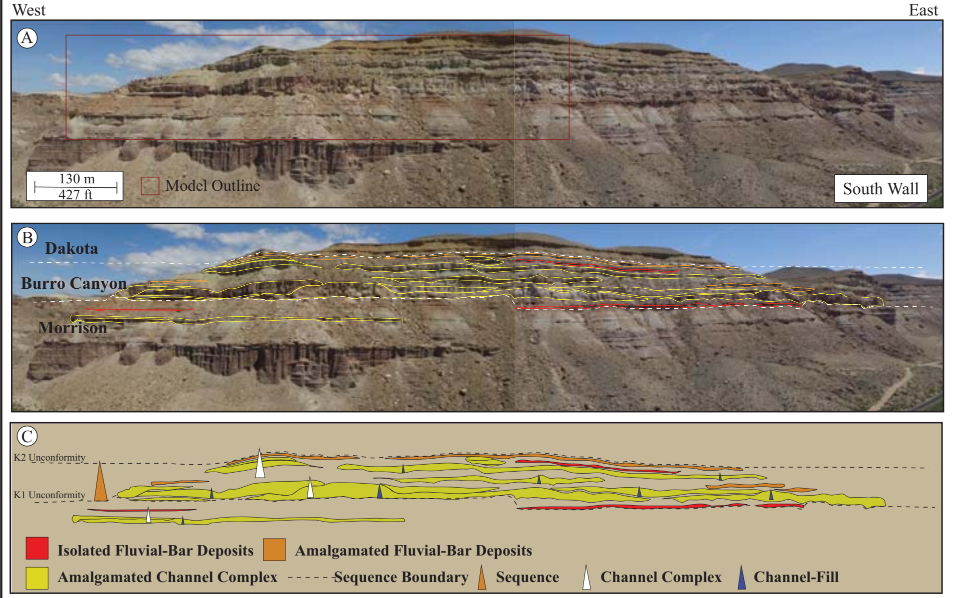

Top: Parallel to paleoflow orientation, red box indicates 2-D model boundary along the southeast wall. Amalgamated channel complex, amalgamated fluival-bar deposits and isolated fluvial-bar deposits compose two indiviual channel complexes present. The lower channel complex is amalgamated and the upper is semi-amalgamated. These two channel complexes represent a single depositional sequence bounded by the K-1 and K-2 unconformities in the Burro Canyon Formation.

Left: Perpendicular to paleoflow orientation, red box indicates 2-D model boundary along the south wall. Amalgamated channel complex, amalgamated fluvial-bar deposits and isolated fluvial-bar deposits compose two indiviual channel complexes present. The lower channel complex is amalgamated and the upper is semi-amalgamated. These two channel complexes represent a single depositional sequence bounded by the K-1 and K-2 unconformities in the Burro Canyon Formation.

2-D Lithofacies Models

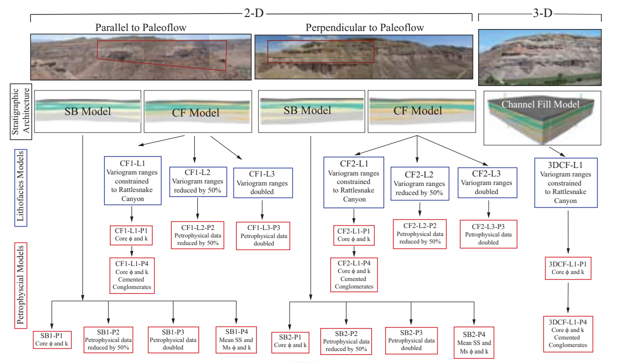

Model workflow showing two- and three-dimensional models created to assess reservoir performance in Rattlesnake Canyon. Two basic 2-D models were created in each orientation to assess reservoir heterogeneity. Within each model, lithofacies models and/or petrophysical models are created in order to test the effects of changing lithofacies and petrophysical variogram ranges on reservoir performance. A single lithofacies model was created in 3-D with two petrophysical models to observe how the reservoir performs in 3-D, both normally and with cemented conglomeratic facies.

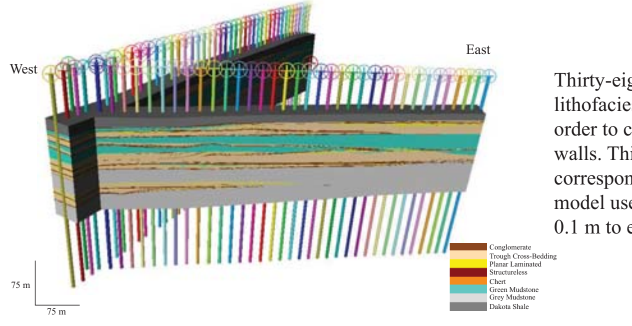

Thirty-eight individual pseudowells and corresponding lithofacies logs were created in each orientation in order to constrain the models to the exposed canyon walls. This creates geometries and lithofacies corresponding with those observed in outcrop. Each model uses 3,000,000 grid cells that are 1 m x 1 m x 0.1 m to ensure fine resolution within models.

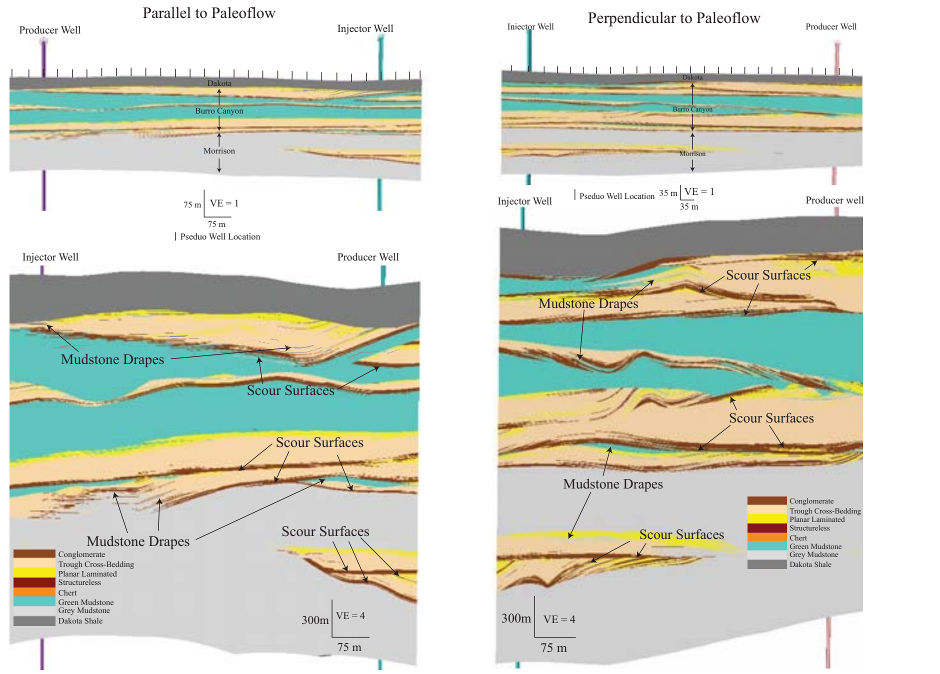

Two-dimensional models oriented parallel and perpendicular to paleoflow. Vertical exaggeration reveals internal heterogeneities preserved within individual models. Scour surfaces annd mudstone drapes are observed creating internal fluid-flow baffles within the reservoir sandstones..

3-D Lithofacies and Petrophysical Models

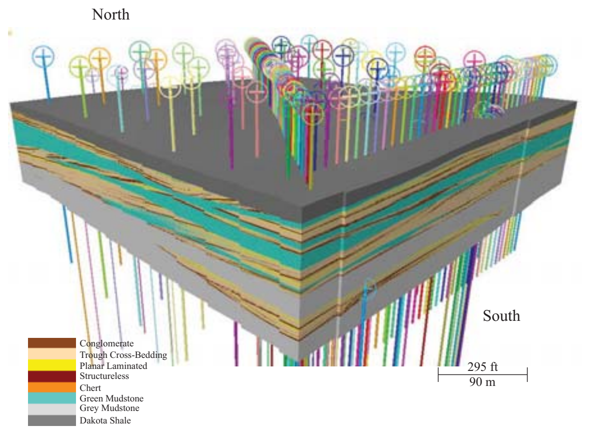

Three-dimensional models were created using 151 pseudo wells. 127 of these pseudo wells are tied directly to outcrop using a 30-foot sspacing along exposed Burro Canyon Formation, remaining 24 wells are used to constrain interior of canyon without exposures present.

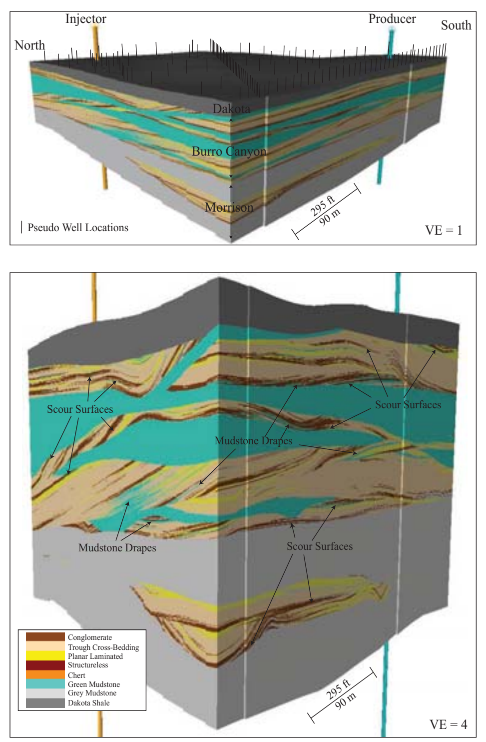

Three-dimensional lithofacies model of the Burro Canyon Formation in Rattlesnake Canyon. Model utilizes ~850,000,000 model grid cells. Grid cells are 1 m x 1 m x 0.1 m. Vertical exaggeration reveals internal heterogeneities preservved with fine scale resolution in model. Scour surfaces and mustone drapes can be seen inside reservoir sandstones creating internal heterogeneity.

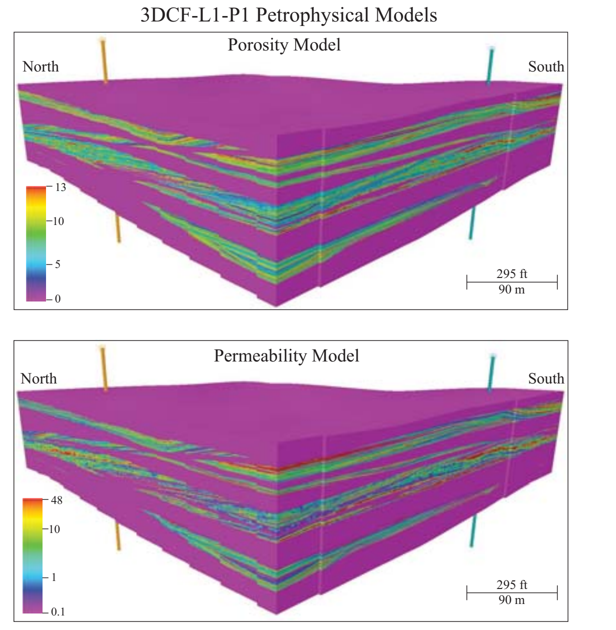

Lithofacies models are populated with petrophysical data from Mitchell Energy Federal 8-1 well. Porosity and permeability values are assigned to individual lithofacies to create the most accurate reservoir model.

2-D Fluid Flow Simulations

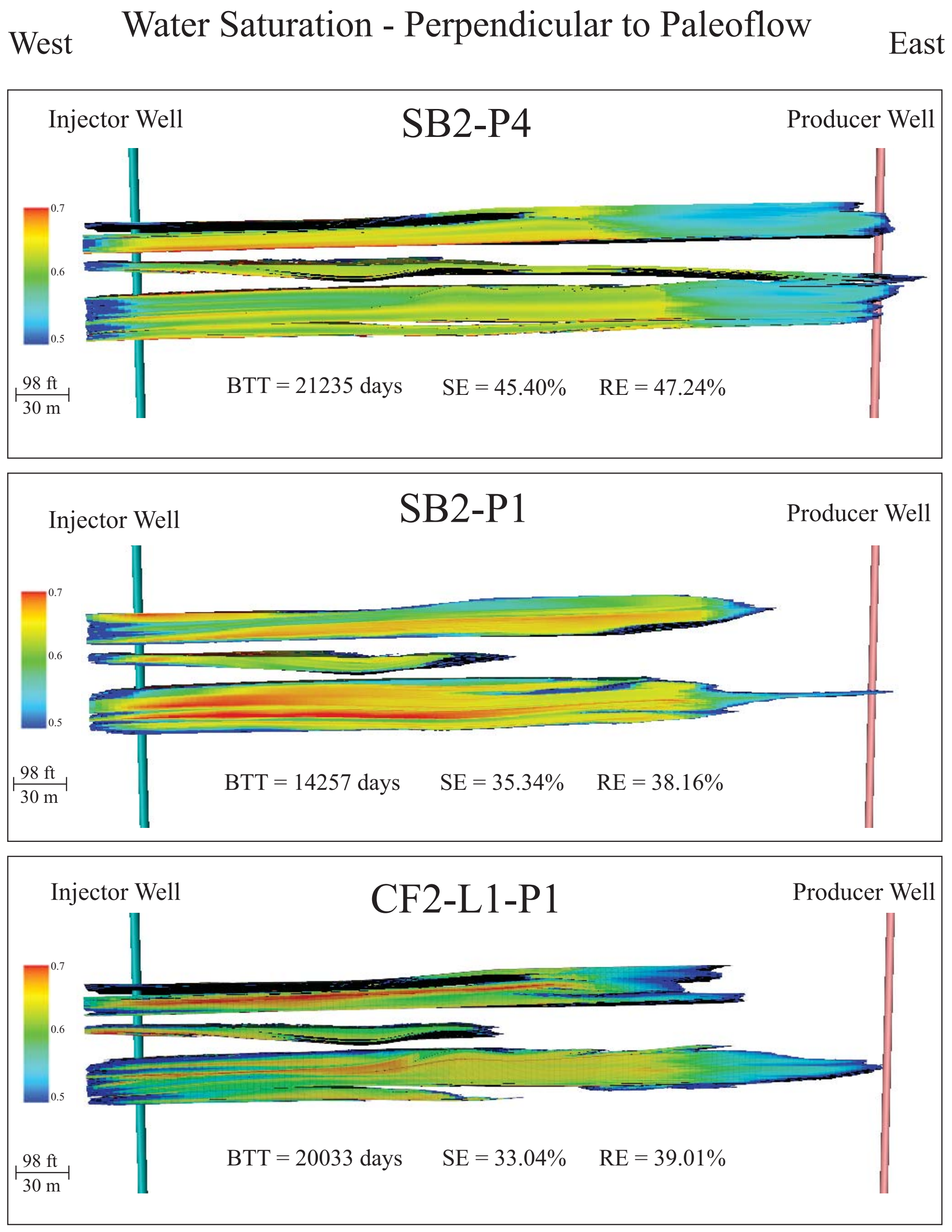

Reservoir models are placed at Burro Canyon Formation subsurface conditions and simulated using a waterflood from an injector to producer well. Simulations were analyzed for breakthrough time (BTT), sweep efficiency (SE) and recovery efficiency (RE)

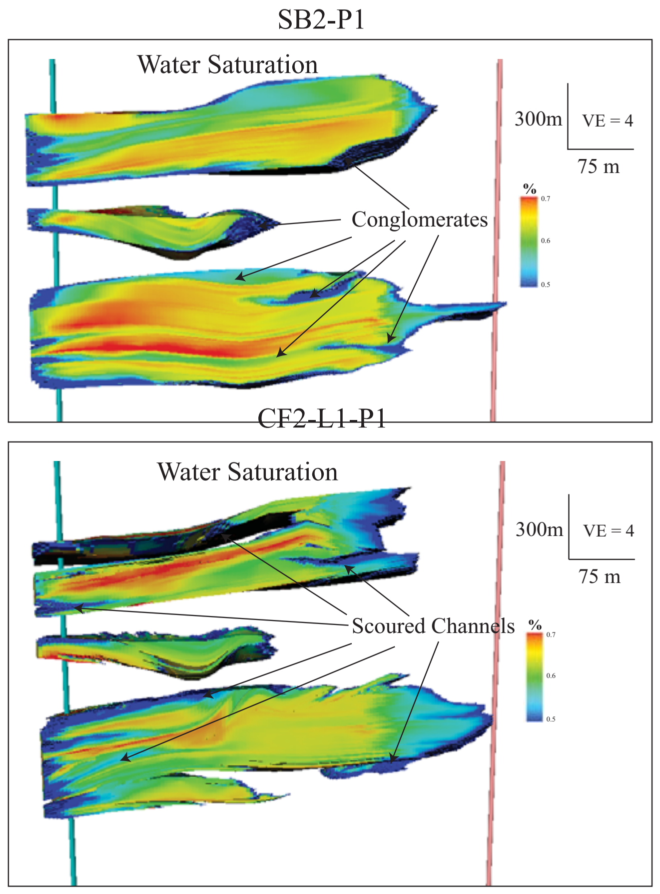

Comparing three levels of internal heterogeneity, SB2-P1 which has no internal heterogeneity, SB2-P4 which uses a "tank" petrophysical distribution, and CF2-L1-P1 the most heterogeneous model, waterflood at breakthrough time is shown. Internal heterogeneity decreases sweep efficiency and recover efficiency while shortening breakthrough time by creating fluid-flow pathways

Vertical exaggeration (VE=4) of simulated models reveals impacts of internal heterogeneities on waterflood. Scoured channels create fluid flow baffles decreasing water saturation at that location. Water saturation in channel-fill model does not distribute as thouroghly as the sandstone-body model.

Results

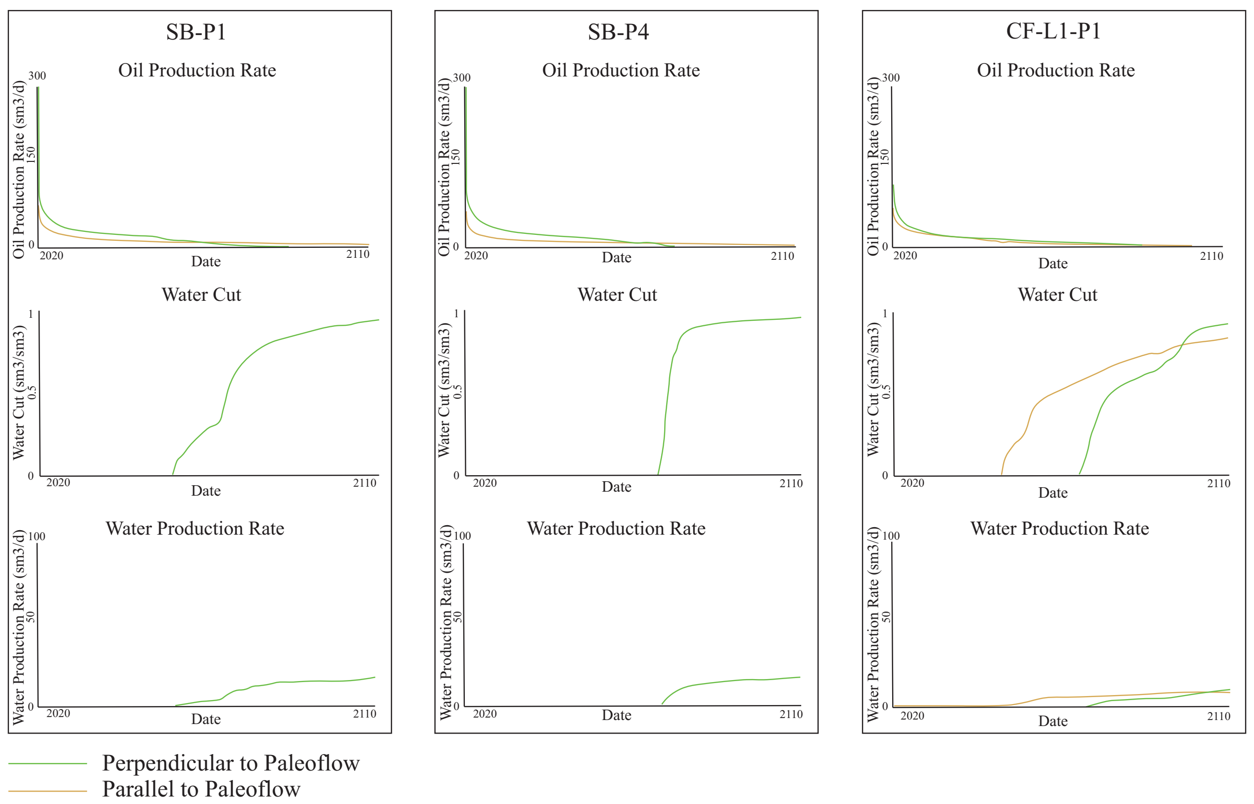

Production charts for the three basic reservoir models with different levels of heterogeneity. Comparison of perpendicular and parallel to paleoflow orientations shows higher connectivity perpendicular to paleoflow resulting in 16% higher sweep efficiency than parallel. Breakthrough times are longer in this orientation.

Results of Breakthrough time (BTT), sweep efficiency (SE) and recovery efficiency (RE) of each simulated model.

SB Models

	BTT Days	RE @ BTT	SE @ BTT	RE @ 100 days	SE @ 100 days
SB2-P1	14257	38%	35%	47%	71%
SB1-P1	+36500	37%	33%	37%	47%
SB2-P2	8786	33%	33%	47%	71%
SB1-P2	16119	33%	33%	40%	68%
SB2-P3	15848	34%	32%	44%	64%
SB1-P3	14319	29%	22%	38%	50%
SB2-P4	21235	47%	45%	49%	75%
SB1-P4	+36500	37%	55%	37%	55%

CF Models

	BTT Days	RE @ BTT	SE @ BTT	RE @ 100 days	SE @ 100 days
CF2-L1-P1	20033	39%	33%	46%	69%
CF1-L1-P1	11721	28%	22%	41%	63%
CF2-L2-P2	9784	32%	26%	47%	70%
CF1-L2-P2	12441	32%	24%	44%	70%
CF2-L3-P3	12879	35%	25%	43%	61%
CF1-L3-P3	10595	30%	21%	39%	61%
CF2-L1-P4	17283	33%	24%	41%	56%
CF1-L1-P4	12271	25%	16%	33%	46%

3-D Models

	BTT Days	RE @ BTT	SE @ BTT	RE @ 100 days	SE @ 120 days
3DCF-L1-P1	47515	24%	24%	25%	40%
3DCF-L1-P4	32141	19%	28%	19%	28%

3-D Fluid-Flow Simulations

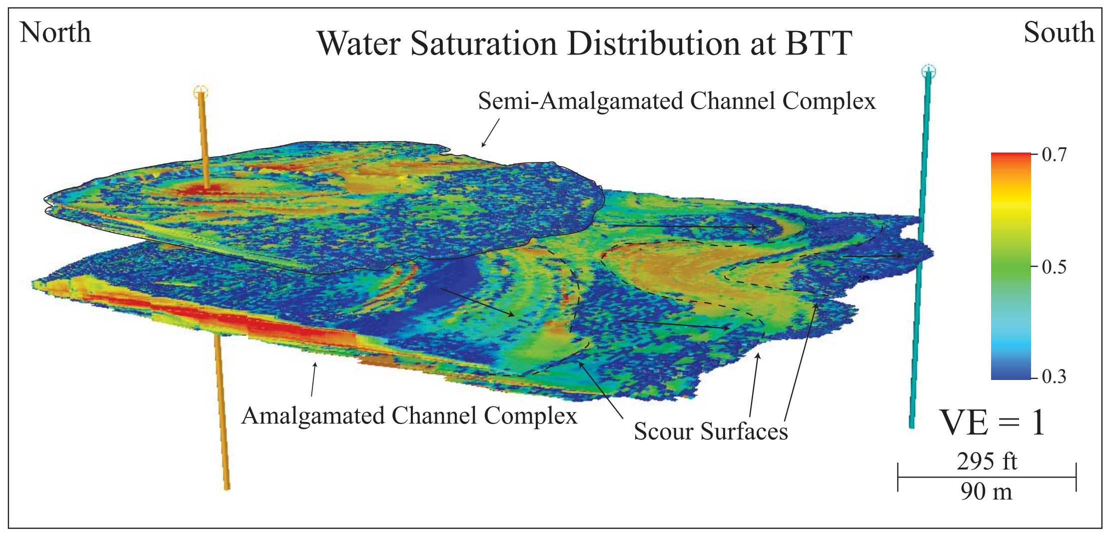

Three-dimensional water saturation model showing distribution of waterflood thorughout the reservoir. Amalgamated channel complex is the most prolific architectural element, providing higher net-to-gross ratios and a larger sandstone body connectivity.

3DCF-L1-P1

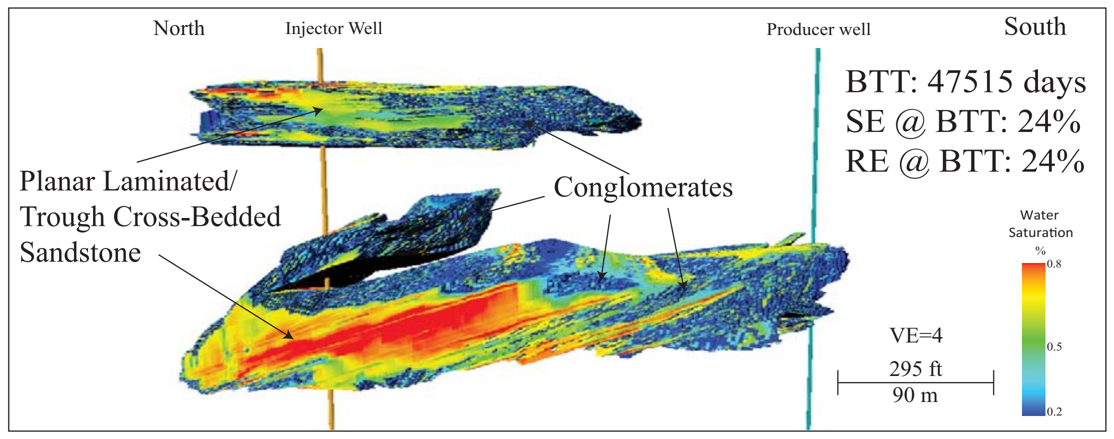

3DCF-L1-P1

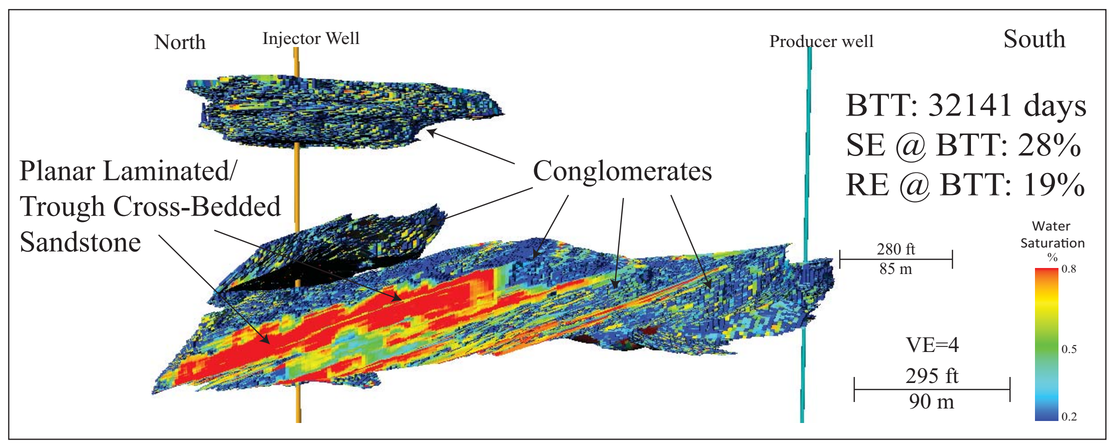

Side view comparison of two simulated 3-D models. Planar laminated and trough cross-bedded sandstone show the highest water saturations in both models, conglomerates shwos singificant decrease in water saturation in cemented model. Extent of the waterflood through the reservoir is lessened in the semi-amalgamated complexes. Sweep efficiency increases by 28%.

3DCF-L1-P1

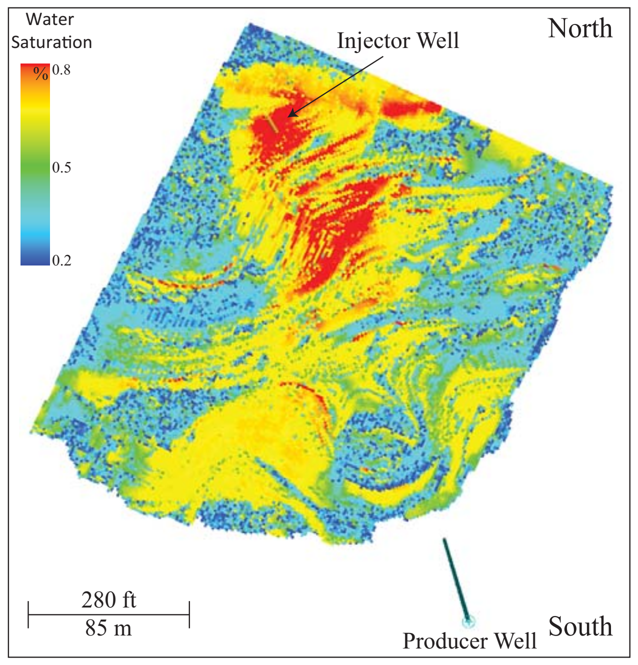

3DCF-L1-P4

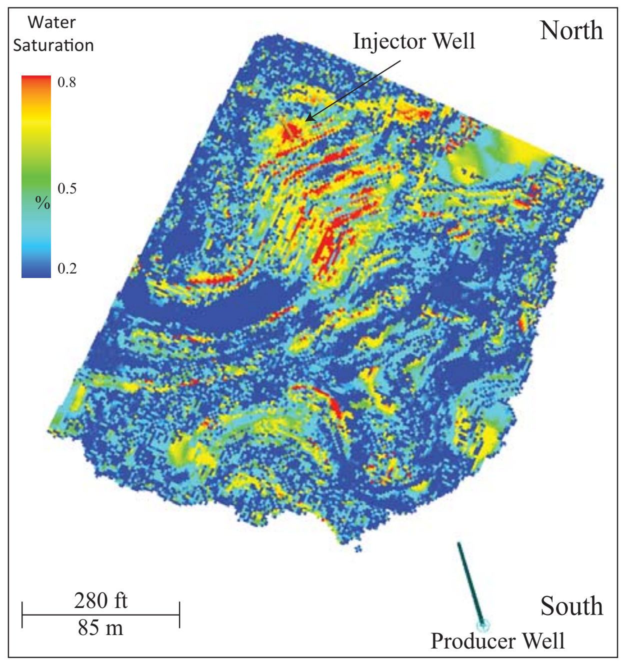

Top view of the two 3-D waterflood simulations performed. Top shows petrophysical distributions from the Mitchell Energy Federal 8-1 well. Bottom shows cemented conglomeratic facies. water saturation of the reservoir significantly decreases when cement is applied. scour surfaces observed contain little to no water saturaiton, reducing fluid flow pathways.

Conclusions

- The Burro Canyon Formation was deposited in a sand-prone, low-sinuosity, braided fluvial environment of the South Saskatchewan type.
- Internal reservoir heterogeneity can account for a 46% shorter breakthrough time and a 21% decrease in sweep efficiency of the reservoir.
- Models oriented perpendicular to paleoflow exhibit higher sweep efficiency (16%) than oriented parallel to paleoflow.
- Changes in lithfoacies variogram ranges have little to no impact on production (~1%)
- Changes in petrophysical variogram ranges have the greatest impact on BTT
- Cement in the reservoir can decrease recovery efficiency by 22% and sweep efficiency by 25% in 2-D and increase sweep efficiency by 28% in 3-D.

Acknowledgements:

Funding for this research was provided by the Reservoir Characterization and Modeling Laboratory. Special thanks to Schlumberger for providing Petrel and Eclipse to create dynamic reservoir models and to Pix4D Mapper Pro for drone-based image modeling.